Ion imaging with a time-of-flight ion computed tomography system based on ultra-fast silicon sensors

The 5th Ion Imaging Workshop, Vienna, Austria
21st October 2024

Felix Ulrich-Pur on behalf of the HADES LGAD group
at GSI and the ion CT group of HEPHY and TU WIEN

Ultra Fast Silicon Detectors/Low Gain Avalanche Diodes

Low Gain Avalanche Diodes (LGADs)

- thin silicon detector optimized for timing performance
  - gain layer exhibits high electric fields ($> 300\,\mathrm{keV/cm}$)
    - leads to intrinsic signal amplification
    - results in large signals with short rise times (< 1 ns)
- why low gain?
  - high gain also amplifies noise
    - leads to temporal signal fluctuations (time jitter)
    - deteriorates time resolution
  - LGADs are operated at controlled low gain ($\approx$ 10-30)
    - to optimize SNR and time resolution

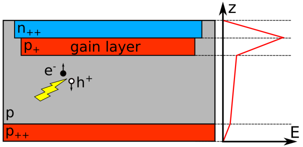

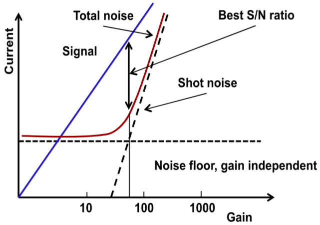

Figure: Sadrozinski et al. 2017

Low Gain Avalanche Diodes (LGADs)

- thin silicon detector optimized for timing performance
  - gain layer exhibits high electric fields ($> 300\,\mathrm{keV/cm}$)
    - leads to intrinsic signal amplification
    - results in large signals with short rise times (< 1 ns)

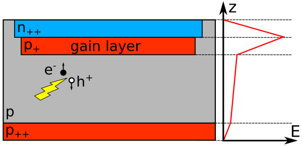

- why low gain?
  - high gain also amplifies noise
    - leads to temporal signal fluctuations (time jitter)
    - deteriorates time resolution
  - LGADs are operated at controlled low gain ($\approx$ 10-30)
    - to optimize SNR and time resolution

$$\sigma_T^2 \approx \underbrace{\left(\frac{T_{rise}}{SNR}\right)^2}_{\sigma_{jitter}^2} + \underbrace{\sigma_{T,floor}^2}_{\text{gain indep.}}$$

Low Gain Avalanche Diodes (LGADs)

- LGADs are promising candidates for 4D-tracking
  - time resolutions down to 30-50 ps possible
  - high spatial resolution ($< 100\,\mu m$)
  - low material budget ($X/X_0 \ll 1\,\%$)
  - radiation hard ($\approx 10^{15} n_{eq}/cm^2$)
  - large sensor areas $\mathcal{O}(cm^2)$
  - high particle rates (e.g. $10^8\ p/s/cm^2$ at HADES)
- high interest in high energy physics community
  - CERN high luminosity upgrade
    - ATLAS High-Granularity Timing Detector (HGTD)
    - CMS Endcap Timing Layer (ETL)
  - HADES T0 detector at GSI
  - beam monitor system at S-DALINAC
  - radiation detector for space applications

HADES T0 detector

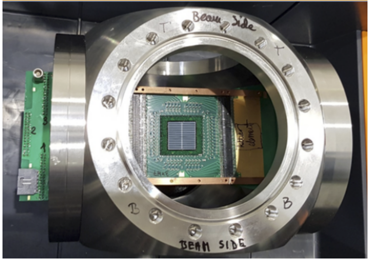

- but also medical applications
  - ion therapy beam quality monitor (Vignati et al. 2023)
  - **ion imaging**

LGAD-based TOF-iCT system

LGAD-based TOF-iCT system - overview

- LGAD-based TOF-iCT system
  - requires 6 4D-tracking layers
  - TOF in air for residual energy determination
  - TOF through object + energy loss for PID (Rovituso et al. 2017)

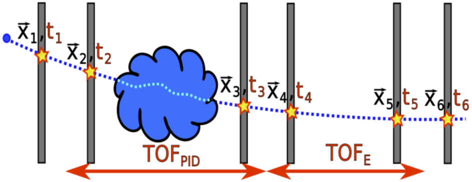

- second approach: “sandwich” TOF-iCT
  - indirect WEPL measurement via TOF through object (Ulrich-Pur 2022)
  - no need for residual energy detector
  - requires only 4 4D-tracking layers
  - compact scanner design

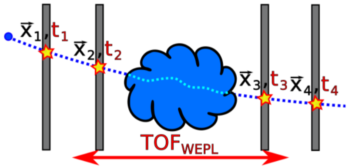

TOF-iCT demonstrator system

TOF-iCT demonstrator - current setup

- TOF-iCT demonstrator at GSI
  - four 1 $\times$ 1 cm^2 FBK strip LGADs with 100 µm pitch
  - discrete front-end electronics
  - FPGA-based TDCs with leading-edge discriminator
    - 4x DIRICH5s1 (32 channels per DiRICH)
  - imaging of small objects $\mathcal{O}(< 1\,\text{cm}^2)$

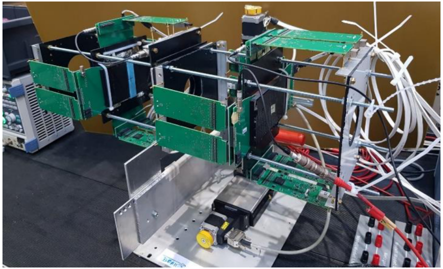

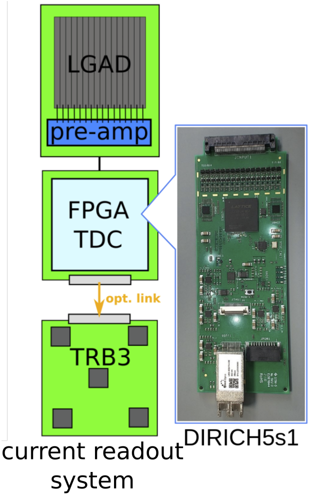

TOF-iCT demonstrator - first experiment

- MedAustron testbeam in April 2023
  - 10^5 p/s protons with 83 and 100.4 MeV
  - 1.6 mm PMMA slabs for WEPL calibration
  - pRad of Al stair phantom was recorded

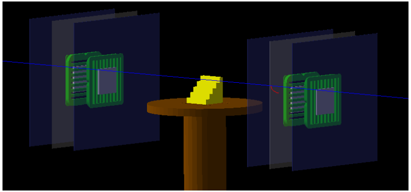

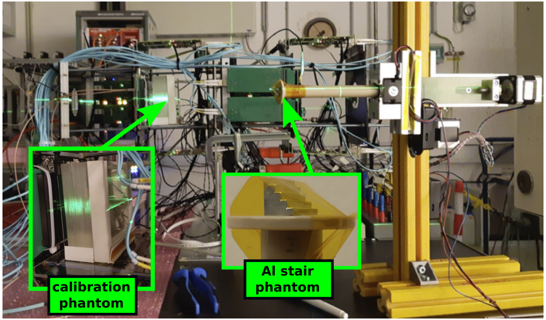

- first experimental TOF-based (Sandwich) pRad: Ulrich-Pur et al. 2024

TOF-iCT demonstrator - WET calibration

- TOF per pixel was measured for different PMMA absorber thicknesses at two different beam energies
- 5th-order polynomial was used to fit the increase in TOF to the corresponding WET

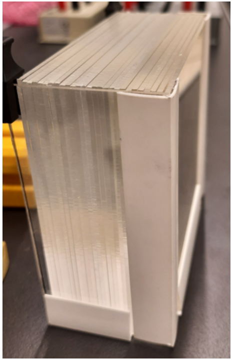

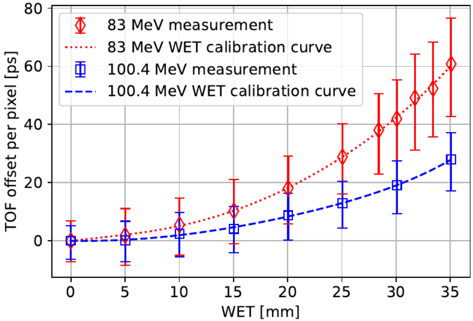

TOF-iCT demonstrator - Sandwich TOF-pRad

- Al stair phantom was mounted on rotational table
  - due to alignment and size of sensors, only part of phantom could be imaged (ROI)
- pRads were recorded at 83 and 100.4 MeV

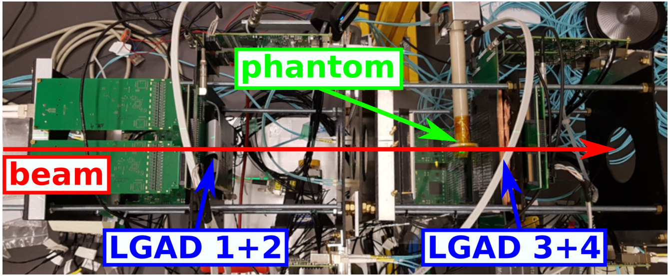

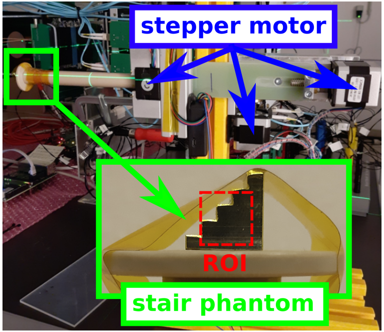

TOF-iCT demonstrator - Sandwich TOF-pRad

- increase in TOF was measured in $0.2 \times 0.2\,\mathrm{mm}^2$ pixels projected onto the last two LGAD planes (i.e. 2×2 LGAD strips per pixel)
  - on last LGAD, only every second channel was connected
- Al stair phantom still clearly visible
  - however, WET overestimated
  - upgrade of setup and improvement of systematic errors is ongoing

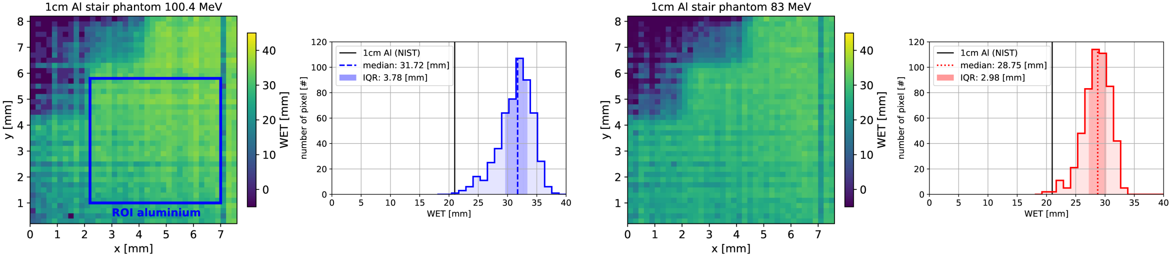

TOF-iCT demonstrator - TOF calorimeter

- second testbeam in June 24
  - TOF-iCT demonstrator operated as TOF calorimeter
  - TOF in air was correlated to beam energy
  - WET measurements were performed
  - different particle rates were tested

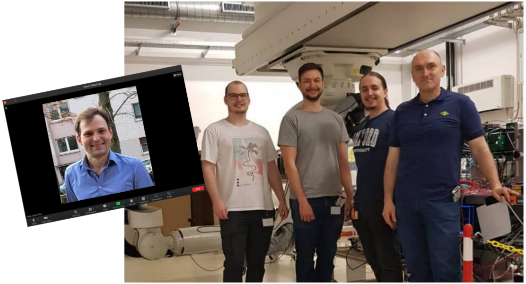

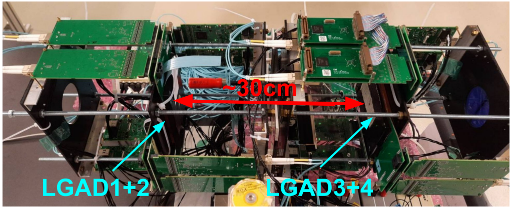

- small changed were made to the TOF-iCT demonstrator
  - added new FPGA TDCs to fully read out all sensors
  - scanner length was increased to 30 cm

TOF-iCT demonstrator - TOF calorimeter

- 1 cm thick CIRS slabs
  - solid water and dense bone were used
  - RSP reference was measured with the PTW Peakfinder

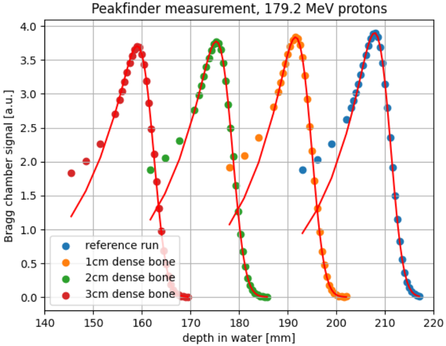

TOF-iCT demonstrator - TOF calorimeter

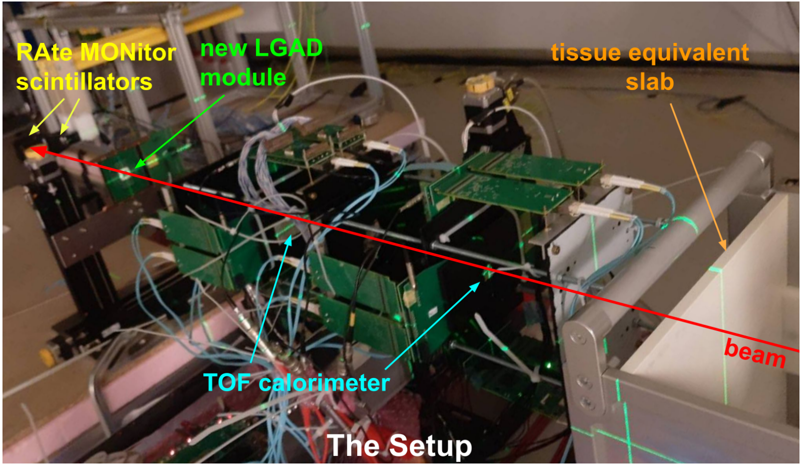

TOF-iCT demonstrator - TOF calorimeter

- energy vs TOF calibration was done prior to WET measurements
  - TOF was determined for beam energies between 62.4 MeV and 252.7 MeV
  - measurements were compared to simulation and TOF in vacuum
- still, systematic errors visible
  - possible tilt of LGADs detected
  - TOF distribution could be used for track-based alignment procedure (WIP)

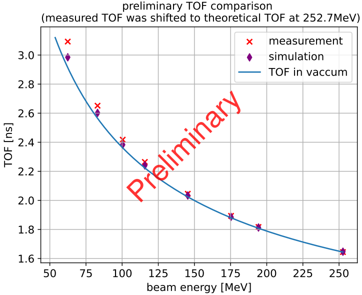

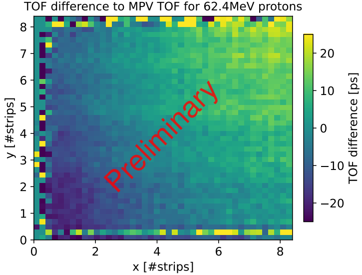

TOF-iCT demonstrator- DAQ speed

- WET accuracy optimization still WIP
- but what about speed?
  - during HADES experiment at GSI 10^8 p/s/cm^2 rising edges were detected
  - at MedAustron, on the other hand, a reduced particle rate was used to provide clean 4D particle tracks $\mathcal{O}(100\,\text{kHz}) - \mathcal{O}(4\,\text{MHz})$ rates)
  - particle rate measured with scintillators matched rates on LGADs
  - however, current DAQ is limited by 100 kHz
- upgraded DAQ is already developed and being tested (DOGMA system)

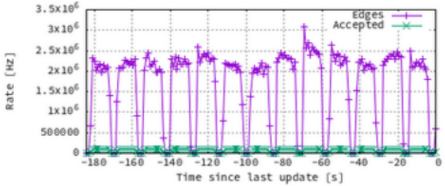

Future and current upgrades for the TOF-iCT demonstrator system

Next version of the ion imaging demonstrator

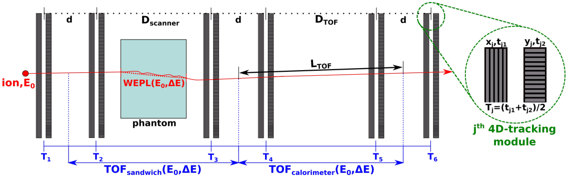

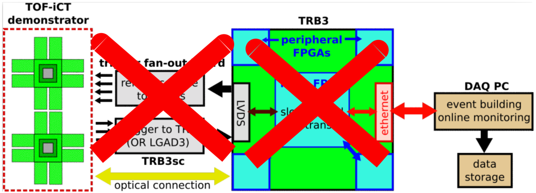

- small, but full TOF-iCT system
  - 12 single-sided LGAD strip sensors with upgraded front-end-electronics
  - DOGMA readout system with optical data transfer

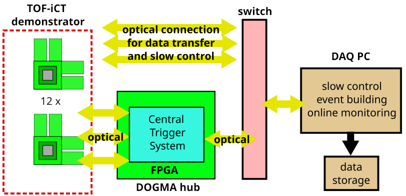

Next version of the ion imaging demonstrator

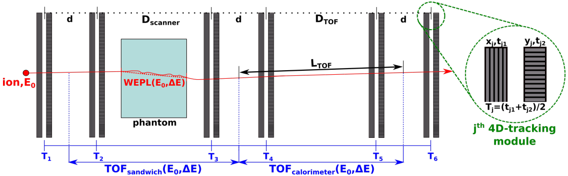

- small, but full TOF-iCT system
  - 12 single-sided LGAD strip sensors with upgraded front-end-electronics
  - DOGMA readout system with optical data transfer

- development and testing of next scanner is part of FWF Erwin Schrödinger grant Nr J 4762-N
  - first 4D-tracking module will be tested soon at MedAustron
  - both Sandwich TOF-iCT and standard TOF-iCT will be investigated with new scanner
  - data sets for Sandwich TOF-iCT will be created

Summary and outlook

Summary

- LGADs are promising 4D-tracking detectors with many applications
  - well-suited for ion imaging
- two different scanner concepts
  - “standard” TOF-iCT system with a TOF calorimeter
  - sandwich TOF-iCT system without a residual energy detector
- TOF-iCT demonstrator system
  - demonstrator system based on LGAD strip sensors was built and tested
  - first sandwich TOF-pRad of an aluminium stair phantom was successfully recorded at MedAustron to show proof-of-principle
  - WET measurements with TOF calorimeter were performed
  - systematics of real experiment are being studied

Outlook

- Sandwich TOF-iCT
  - WEPL calibration algorithms will be further optimized
  - semi-analytical approach in development (Stephan Kwas)
  - STOFICT project by CREATIS recently received funding (Simon Rit et al.)
- short-term goal
  - improvement of current demonstrator system
  - further measurements with demonstrator system planned
- future large-area system
  - requires dedicated ASIC which can handle high rates and large number of channels
  - dedicated module design to build low-mass large area system

Thank you for your attention!

- **TU WIEN/HEPHY**
  - Thomas Bergauer
  - Andreas Gsponer
  - Albert Hirtl
  - Matthias Kausel (MedAustron)
  - Daniel Makay
  - Stephan Kwas
- **GSI**
  - Tetyana Galatyuk
  - Vadym Kedych
  - Yevhen Kozymka
  - Wilhelm Krüger
  - Jerzy Pietraszko
  - Adrian Rost
  - Christian Joachim Schmidt
  - Michael Träger
  - Michael Traxler
- **FBK**
- **CREATIS**

This research was funded in whole or in part by the Austrian Science Fund (FWF) Erwin-Schrödinger Grant Nr. J 4762-N

Backup

Future large-area 4D-tracking system

Community Input for NuPECC Long Range Plan 2024

Ultra-fast silicon detectors for nuclear physics and medical applications

Felix Ulrich-Pur[1], Anton Andronic[2], Thomas Bergauer[3], Maurizio Boscardin[4], Michael Deveaux[1], Tetyana Galatyuk[1,6,7], Albert Hirtl[5], Jan Michel[8], Alexandre Obertelli[6,7], Jerzy Pietraszko[1], Adrian Rost[9], Christian Schmidt[1], Joachim Stroth[1,7,8], Michael Traxler[1], Matteo Centis Vignali[4], Marc Weber[10], Christian Wendisch[1]

[1]GSI Helmholtzzentrum für Schwerionenforschung GmbH, Germany
[2]Institut für Kernphysik, Universität Münster, Germany
[3]Österreichische Akademie der Wissenschaften, Austria
[4]Fondazione Bruno Kessler, Italy
[5]Technische Universität Wien, Austria
[6]Institut für Kernphysik, Technishe Universität Darmstadt, Germany
[7]Helmholtz Forschungsakademie Hessen für FAIR, Germany
[8]Goethe Universität Frankfurt, Germany
[9]Facility for Antiproton and Ion Research in Europe GmbH, Germany
[10]Karlsruhe Institute of Technology, Germany

Future large-area 4D-tracking system

- novel LGAD sensors with increased fill factor will be investigated
  - new sensor production with trench-isolated LGADs planned
- upgraded readout electronics with increased number of readout channels
  - dedicated ASIC and FPGA-based TDCs
- dedicated low-mass module design for large active areas (tens of cm^2)
  - low mass flex cables to reduce overall material budget ($X/X_0 < 1\,\%$)

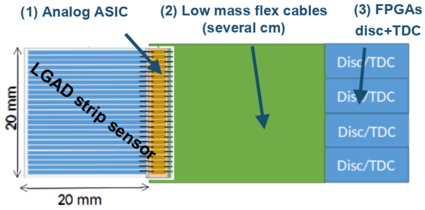

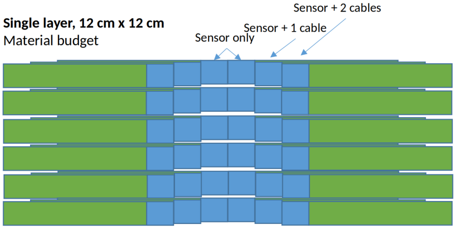

LGAD-based TOF-iCT system - previous work

- Monte Carlo feasibility study (Ulrich-Pur et al. 2022)
  - realistic model of LGAD-based TOF-iCT system
    - assessment of image quality using the CTP404 phantom
    - study of RSP accuracy and resolution
    - RSP MAPE down to 0.12 %
    - time resolution $\leq$ 30-50 ps required
  - see also Krah et al. 2022

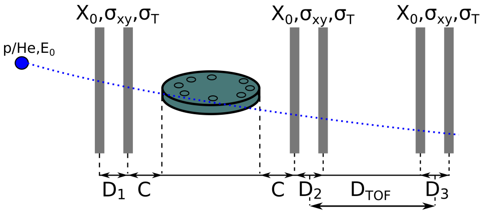

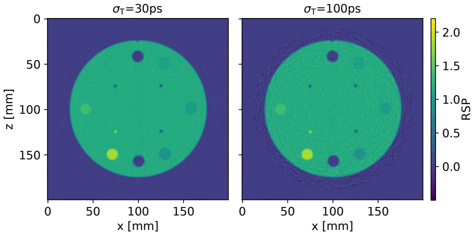

"Sandwich" TOF-iCT - previous work

- Monte Carlo feasibility study (Ulrich-Pur et al. 2023)
  - same MC model as in "standard" TOF-iCT study
  - determine influence of different system parameters on image quality
    - influence on RSP accuracy and resolution
    - measured with CTP 404 phantom
  - first study based on simple WEPL calibration approach to show proof-of-principle
    - WEPL estimation needs still further optimization
    - semi-analytical method currently under investigation

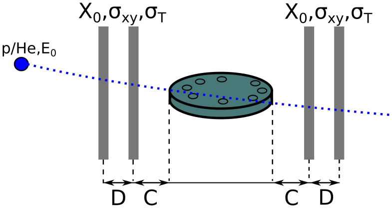

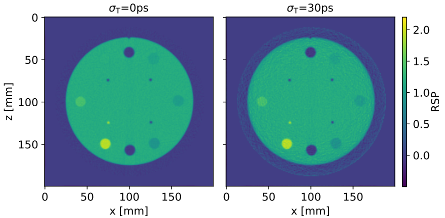

LGAD-based TOF-iCT system - previous work

- Monte Carlo feasibility studies (Ulrich-Pur et al. 2022)
  - see LLU workshop 2021
  - performance study of stand-alone TOF calorimeter
    - influence of system parameters on energy resolution and accuracy
    - implementation of dedicated calibration procedure
    - time resolution 30-50 ps required
    - energy modulation, length of the calorimeter and number of LGADs can be adjusted to optimize the time resolution

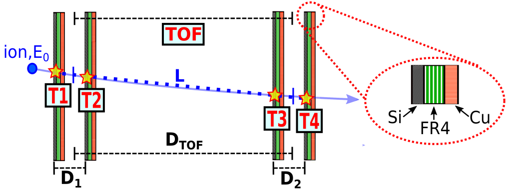

$$E_{\mathrm{kin}} = m_0 c^2 \left(\frac{1}{\sqrt{1 - \frac{L^2}{c^2} \mathrm{TOF}^2} - 1} \right)$$

“Sandwich” TOF-iCT - previous work

- first proof-of-principle measurement at MedAustron in 2021 (Krüger et al. 2022)
  - 4 LGAD strip sensors (HADES) with different geometries
    - total active area: $0.5 \times 0.5\,\mathrm{cm}^2$
  - $100.4\,\mathrm{MeV}$ protons with $\approx 5 \times 10^6\,\mathrm{p/s}$
  - increase in TOF for different PMMA absorbers

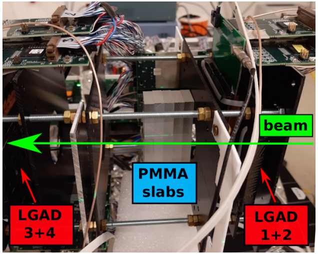

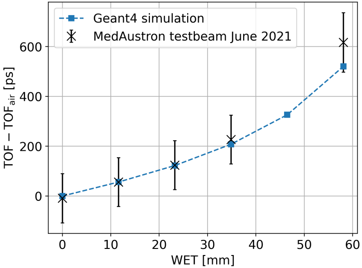

“Sandwich” TOF-iCT - motivation

- main idea:
  - particles loose energy along their path
    - TOF increases depending on traversed material and beam energy
  - find method to exploit increase in TOF through object for WEPL estimation
    - define “new” material dependent quantity, i.e. slowing down power (SDP)
    - define imaging problem
    - find method to map the SDP to the stopping power (SP)

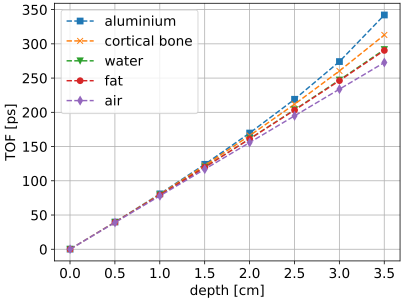

$$\mathrm{TOF} = \int_0^L \frac{\mathrm{d}s}{v(\vec{\mathbf{x}}(s))} \neq \frac{L}{v}$$

- definition of “slowing down power”
  - increase in TOF with respect to the TOF in vacuum per unit path length

$$\mathrm{SDP}(E_{\mathrm{kin}}(\vec{\mathbf{x}}(s)) := \frac{\mathrm{TOF}-\mathrm{TOF}_{\mathrm{vac}}}{\Delta s}(E_{\mathrm{kin}}(\vec{\mathbf{x}}(s))$$

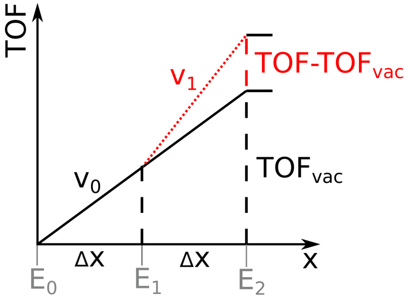

- SDP is directly related to SP

$$\mathrm{SDP}(E(x)) \approx -\frac{\Delta x}{2v^2(E(x))} v'(E(x)) \cdot \mathrm{SP}(E(x))$$

“Sandwich” TOF-iCT - concept

- define relative slowing down power (RSDP)
  - RSDP is approximately equal to the RSP
  - WEPL definition stays the same

$$\text{RSDP} := \frac{\text{SDP}_{\text{mat}}(E(x))}{\text{SDP}_{\text{H}_2\text{0}}(E(x))} \approx \text{RSP}$$

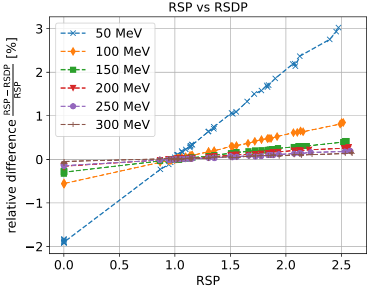

- inverse problem

$$\text{WEPL} := \int_0^{\text{TOF}-\text{TOF}_{\text{vac}}} \frac{\text{d}\Delta\text{TOF}}{\text{SDP}_{H_2\text{0}}(\Delta\text{TOF}(E(\vec{\mathbf{x}}(s))))} = \int_0^L \text{RSDP}\,(\vec{\mathbf{x}}(s))\,\text{d}s \approx \int_0^L \text{RSP}\,(\vec{\mathbf{x}}(s))\,\text{d}s$$

“Sandwich” TOF-iCT - concept

- measuring increase in TOF w.r.t vacuum is challenging
  - requires accurate velocity map to determine TOF in vacuum
  - can be obtained e.g. via MC simulations
- simpler approach
  - measure TOF increase w.r.t TOF in air and calibrate against WEPL
  - use e.g. 5th-order polynomial for calibration

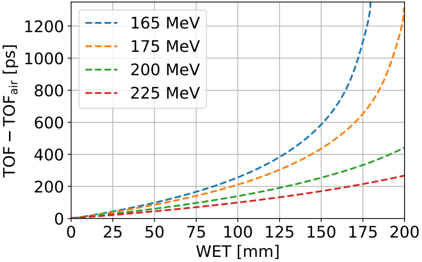

$$\mathrm{TOF} - \mathrm{TOF}_{\mathrm{air}}(\mathrm{WEPL}, \mathrm{E}_0) \approx \sum_{i=0}^{5} a_i(E_0) \cdot \mathrm{WEPL}^i$$

Sandwich TOF-iCT

TOF in matter

$$\mathrm{TOF} = \int_0^L \frac{\mathrm{d}s}{v(\mathbf{x}(s))} = \int_0^L \frac{\mathrm{d}s}{c\,\frac{E_{\mathrm{kin}}(\mathbf{x}(s))}{E_{\mathrm{kin}}(\mathbf{x}(s))+m_0c^2}\sqrt{1+2\frac{m_0c^2}{E_{\mathrm{kin}}(\mathbf{x}(s))}}}$$

- depends on traversed material and beam energy

Increase in TOF

$$\Delta\mathrm{TOF} = \mathrm{TOF} - \mathrm{TOF}_{\mathrm{vac}} = \int_0^{\Delta x} \frac{\mathrm{d}s}{v(\mathbf{x}(s))} - \frac{\Delta x}{v(\mathbf{x}(s{=}0))}$$

- define slowing down power to describe the material dependent increase in TOF

TOF in matter for $L = 2\Delta x$

$$\mathrm{TOF} = \frac{\Delta x}{v(E(x))} + \frac{\Delta x}{v(E(x+\Delta x))}$$

1st-order Taylor expansion

$$\mathrm{TOF} \approx \frac{2\Delta x}{v(E(x))} - \frac{\Delta x^2}{v^2(E(x))}\frac{\partial v(E(x))}{\partial x}$$

TOF in vacuum

$$\mathrm{TOF}_{vac} = \frac{2\Delta x}{v(E(x))}$$

increase in TOF

$$\mathrm{TOF} - \mathrm{TOF}_{vac} \approx -\frac{\Delta x^2}{v^2(E(x))}\frac{\partial v(E(x))}{\partial x}$$

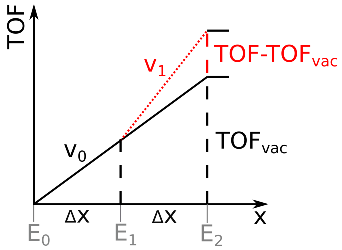

Figure: SDP definition

Slowing down power

$$\mathrm{SDP}(E_{kin}(\mathbf{x}(s))) := \frac{\mathrm{TOF}-\mathrm{TOF}_{vac}}{\Delta s}(E_{kin}(\mathbf{x}(s)))$$

Sandwich TOF-iCT

SDP for $L = 2\Delta x$

$$\mathrm{SDP}(E(x)) = \frac{\mathrm{TOF} - \mathrm{TOF}_{\mathrm{vac}}}{2\Delta x} \approx -\frac{\Delta x}{2v^2(E(x))} \frac{\partial v(E(x))}{\partial x}$$

approximation of derivative

$$\frac{\partial v(E(x))}{\partial x} = \frac{\partial v(E(x))}{\partial E(x)} \frac{\partial E(x)}{\partial x} \approx v'(E(x)) \cdot \mathrm{SP}(E(x))$$

using

$$\frac{\partial E(x)}{\partial x} \approx \mathrm{SP}(E(x)) \; and \; v'(E(x)) = \frac{\partial v(E(x))}{\partial E(x)}$$

relation SDP and SP

$$\mathrm{SDP}(E(x)) \approx -\frac{\Delta x}{2v^2(E(x))} v'(E(x)) \cdot \mathrm{SP}(E(x))$$

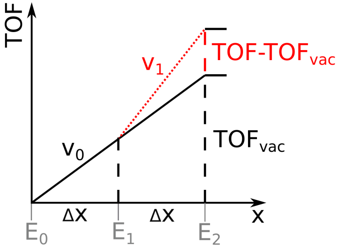

Figure: SDP definition

Slowing down power

$$\mathrm{SDP}(E_{\mathrm{kin}}(\mathbf{x}(s))) := \frac{\mathrm{TOF} - \mathrm{TOF}_{\mathrm{vac}}}{\Delta s}(E_{\mathrm{kin}}(\mathbf{x}(s)))$$

Relative slowing down power (RSDP)

$$\text{RSDP} := \frac{\text{SDP}_{\text{mat}}(E(x))}{\text{SDP}_{\text{H}_2\text{0}}(E(x))}$$

RSDP vs RSP

$$\text{RSDP} \approx \frac{-\frac{\Delta x}{2v^2(E(x))} v'(E(x)) \cdot \text{SP}_{\text{mat}}(E(x))}{-\frac{\Delta x}{2v^2(E(x))} v'(E(x)) \cdot \text{SP}_{\text{H}_2\text{0}}(E(x))} = \text{RSP}$$

- RSDP is approximately equal to RSP
- WEPL definition is also the same

WEPL

$$\text{WEPL} = \int_0^L \text{RSP}(\mathbf{x}(s)) \approx \int_0^L \text{RSDP}(\mathbf{x}(s))\, ds$$

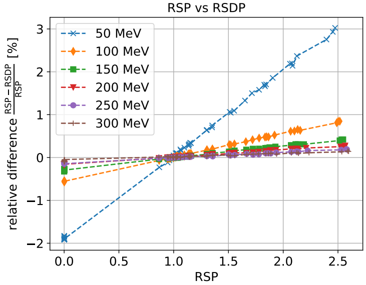

Figure: RSP error

RSDP vs RSP

$$\text{RSDP} := \frac{\text{SDP}_{\text{mat}}(E(x))}{\text{SDP}_{\text{H}_2\text{0}}(E(x))} \approx \text{RSP}$$

Imaging problem

$$\text{WEPL} := \int_0^{\text{TOF}-\text{TOF}_{\text{vac}}} \frac{\text{d}\Delta\text{TOF}}{\text{SDP}_{H_20}(\Delta\text{TOF}(E(\mathbf{x}(s))))} = \int_0^L \text{RSDP}\,(\mathbf{x}(s))\,\text{d}s \approx \int_0^L \text{RSP}\,(\mathbf{x}(s))\,\text{d}s$$

Measuring increase in TOF w.r.t vacuum is challenging

- requires accurate velocity map to determine TOF in vacuum
  - can be obtained e.g. via MC simulations

Simpler approach

- measure TOF increase w.r.t TOF in air and calibrate against WEPL
  - use e.g. 5th-order polynomial for calibration

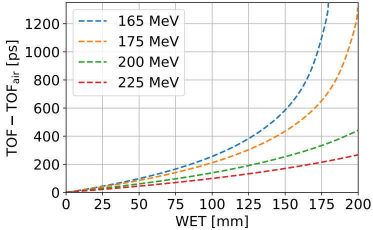

$$\text{TOF} - \text{TOF}_{\text{air}}(\text{WEPL}, \text{E}_0) \approx \sum_{i=0}^{5} a_i(E_0) \cdot \text{WEPL}^i$$

- RSP resolution (QCOD) shows similar dependence on time resolution and beam energy when compared to standard TOF-iCT system
- RSP accuracy $\geq 0.91\,\%$
  - still shows systematic dependence on system parameters
    - more dedicated calibration procedure/model is currently under investigation

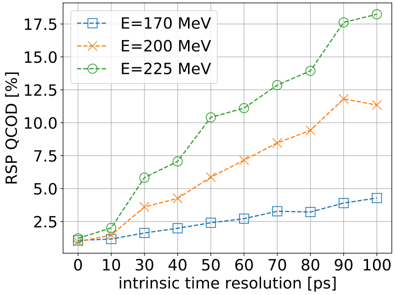

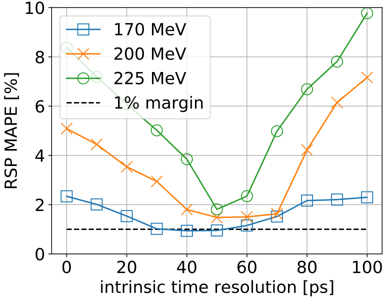

explanation of u-shape of MAPE

- RSP is generally overestimated (positive RSP error)
  - skewed TOF distribution results in shift towards higher TOF and therefore WET values
  - caused by non-straight paths (MCS) etc.
- intrinsic time resolution compensates for this effect
  - time measurement error results in asymmetric shift on WET distribution (last slide)
  - shifted towards lower WET values
  - RSP error decreases and becomes negative

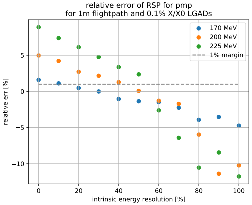

Figure: rel. err in PMP

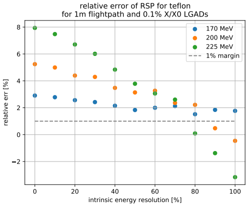

Figure: rel. err in Teflon

Time resolution of LGADs

- final time resolution depends on every step in the readout chain

$$\sigma_T^2 = \sigma_{\text{time walk}}^2 + \sigma_{\text{Landau noise}}^2 + \sigma_{\text{distortion}}^2 + \sigma_{\text{jitter}}^2 + \sigma_{\text{TDC}}^2$$

$\sigma_{\text{TDC}}^2 \rightarrow \Delta T/\sqrt{12}$

digitization

irregularities in signal shape due to energy loss fluctuations

detector geometry (e.g. segmentation) can result in position dependent drift velocity and Weighting fields and therefore to signal shape variations
$i \propto qvE_w$

sensor and electronics noise

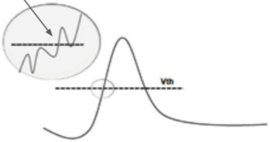

Image: (Sadrozinski et al., 2020)

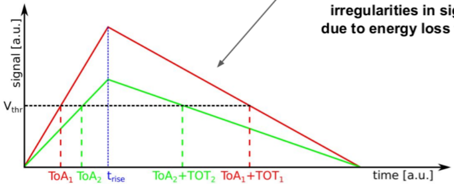

varying signal amplitude (time walk effect)

TOF-iCT demonstrator - sensor calibration

- precise time measurements require precise sensor calibration
  - calibration of constant threshold signal discrimination (time-walk effect)
  - synchronisation of all LGAD channels per 4D-tracking module (offset correction)
- time-walk and offset correction was performed for each LGAD channel

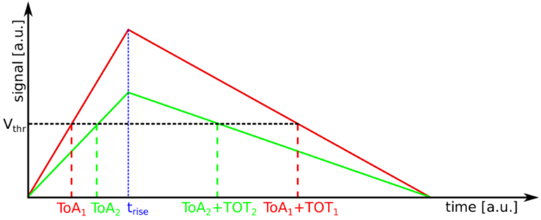

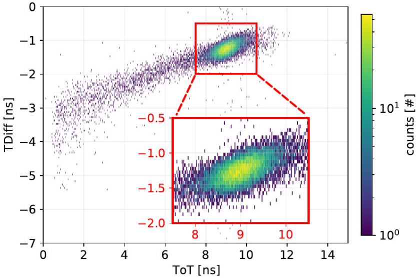

TOF-iCT demonstrator - sensor calibration

- precise time measurements require precise sensor calibration
  - calibration of constant threshold signal discrimination (time-walk effect)
  - synchronisation of all LGAD channels per 4D-tracking module (offset correction)
- time-walk and offset correction was performed for each LGAD channel

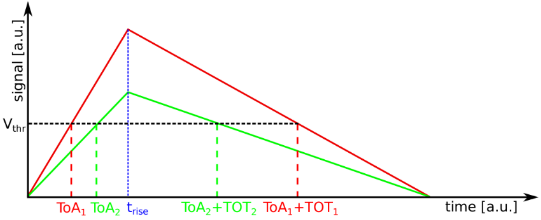

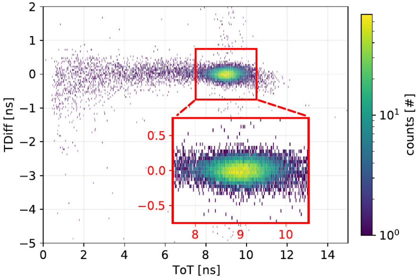

TOF-iCT demonstrator - sensor performance

- TOF and intrinsic time resolution was measured for different beam energies and every LGAD channel
  - time resolution improves with lower beam energy due to higher signal in detector
  - needs to be considered in simulations

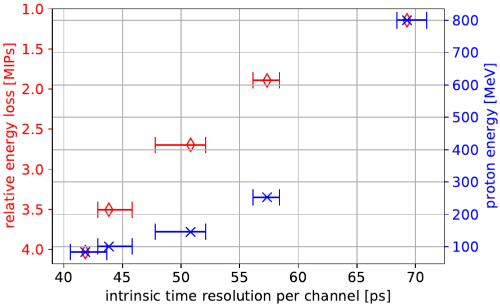

HADES T_0 detector

- LGADs for beam monitoring (Krüger et al. 2022)

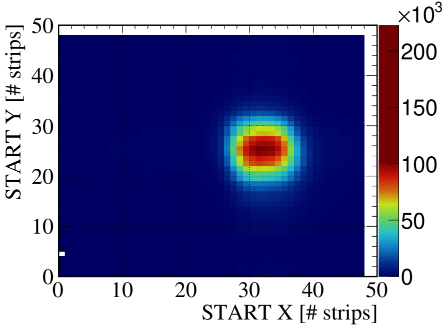

Figure: beam spot measurement

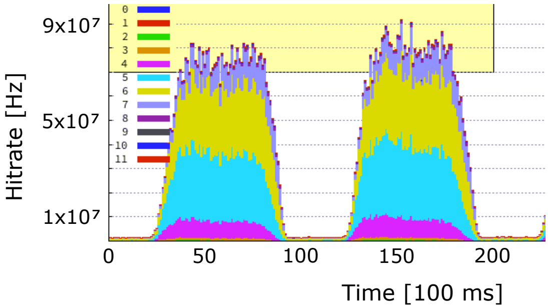

Figure: macro spill structure of p beam

TOF-iCT demonstrator - next steps

- current setup consists of only 2 4D-tracking layers
  - allows only straight-line approximation
- upgrade of current setup with more layers planned (Erwin-Schrödinger grant)
  - main goal: record first TOF-based iCT
  - additional 4D-tracking layers will allow implementation of MLP
  - more experimental data for TOF through matter will be recorded to further test and improve sandwich TOF-iCT models

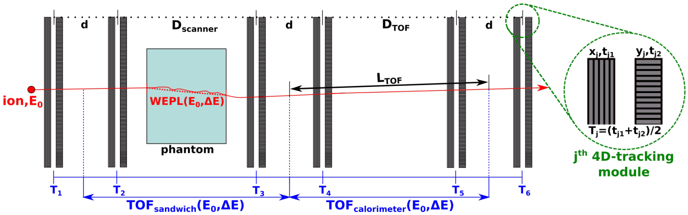

References I

- Krah, Nils et al. (2022). "Relative stopping power resolution in time-of-flight proton CT". In: *Physics in Medicine and Biology* 67.16, p. 165004. DOI: 10.1088/1361-6560/ac7191. URL: https://doi.org/10.1088/1361-6560/ac7191.
- Krüger, W. et al. (2022). "LGAD technology for HADES, accelerator and medical applications". en. In: *Nuclear Instruments and Methods in Physics Research Section A: Accelerators, Spectrometers, Detectors and Associated Equipment* 1039, p. 167046. ISSN: 01689002. DOI: 10.1016/j.nima.2022.167046.
- Rovituso, M et al. (2017). "Fragmentation of 120 and 200 MeV u-14He ions in water and PMMA targets". In: *PMB* 62.4, pp. 1310–1326. DOI: 10.1088/1361-6560/aa5302.
- Sadrozinski, Hartmut F-W et al. (2017). "4D tracking with ultra-fast silicon detectors". In: *Reports on Progress in Physics* 81.2, p. 026101. DOI: 10.1088/1361-6633/aa94d3.

References II

- Ulrich-Pur, F. et al. (2023). “Novel ion imaging concept based on time-of-flight measurements with low gain avalanche detectors”. In: *Journal of Instrumentation* 18.02, p. C02062. DOI: 10.1088/1748-0221/18/02/C02062.
- Ulrich-Pur, Felix (2022). “Advancing Ion Computed Tomography by Incorporating Time-Of-Flight and 4D Tracking”. PhD thesis. DOI: 10.34726/HSS.2022.62102.
- Ulrich-Pur, Felix et al. (2022). “Feasibility study of a proton CT system based on 4D-tracking and residual energy determination via time-of-flight”. In: *Physics in Medicine & Biology*. ISSN: 0031-9155, 1361-6560. DOI: 10.1088/1361-6560/ac628b.
- Ulrich-Pur, Felix et al. (2024). “First experimental time-of-flight-based proton radiography using low gain avalanche diodes”. In: *Physics in Medicine and Biology* 69.7, p. 075031. ISSN: 1361-6560. DOI: 10.1088/1361-6560/ad3326.
- Vignati, Anna et al. (2023). “Calibration method and performance of a time-of-flight detector to measure absolute beam energy in proton therapy”. In: *Medical Physics*. DOI: 10.1002/mp.16637.